

phys. stat. sol. (b) 88, 73 (1978)

Subject classification: 13.2 and 14.3; 15; 22.4.4

Institute of Physics, Polish Academy of Sciences, Warsaw¹⁾

Influence of Exchange Interaction on the Quantum Transport Phenomena in $\text{Hg}_{1-x}\text{Mn}_x\text{Te}$

By

M. JACZYŃSKI, J. KOSSUT, and R. R. GALĄZKA

A series of anomalous features of the Shubnikov-de Haas effect in n-type $\text{Hg}_{1-x}\text{Mn}_x\text{Te}$ mixed crystals is detected, e.g., strong temperature dependence of the ShdH peak positions, large values of electronic g -factors, non-monotonic behaviour of the amplitude of ShdH oscillations as a function of temperature. These features cannot be explained with the help of usual theoretical models. They are explained within the modified Pidgeon-Brown model including the exchange interaction between conduction electrons and electrons from 3d shell of Mn ions. The quantum oscillations of the thermoelectric power are also observed. The behaviour of amplitude and peak positions of thermoelectric power are compatible with those of magnetoresistance.

Eine Reihe von anomalen Merkmalen des Shubnikov-de Haas-Effekts in n-leitenden $\text{Hg}_{1-x}\text{Mn}_x\text{Te}$ -Mischkristallen wird gefunden, z. B. eine starke Temperaturabhängigkeit der Lage des ShdH-Maximums, große Werte des elektronischen g -Faktors, nichtmonotones Verhalten der Amplitude der ShdH-Oszillationen als Funktion der Temperatur. Diese Merkmale lassen sich nicht mit den üblichen theoretischen Modellen erklären. Sie werden mit dem modifizierten Pidgeon-Brown-Modell erklärt, wobei Austauschwechselwirkung zwischen Leitungselektronen und Elektronen aus der 3d-Schale der Mn-Ionen berücksichtigt wird. Quantenoszillationen der Thermospannung werden ebenfalls beobachtet. Das Verhalten der Amplitude und der Lagen des Maximums der Thermospannung sind mit denen der Magnetowiderstandsänderungen vereinbar.

1. Introduction

The mixed crystals of $\text{Hg}_{1-x}\text{Mn}_x\text{Te}$ are solid solutions formed by a zero-gap semiconductor HgTe and a magnetic semiconductor MnTe. Although MnTe and HgTe crystallize in different structures (MnTe — structure of NiAs, HgTe — zincblende structure) the solid solutions can be obtained and their crystal structure is that of zincblende up to $x \approx 0.4$ [1]. These mixed crystals exhibit paramagnetic properties [2, 3], at least in the composition range studied up to now. The band structure of $\text{Hg}_{1-x}\text{Mn}_x\text{Te}$ was studied [4 to 6] in weak magnetic fields and/or at high temperatures (≈ 300 K). These investigations revealed no anomalous features. In particular, no influence of magnetic ions on the band structure was observed. It turned out that the band structure may be described with the help of Kane's theory [7]. The energy distance between Γ_6^- and Γ_8^- levels varies with the composition, as it does in all semiconducting mixed crystals. This variation is presented in Fig. 1. The band ordering is

¹⁾ Al. Lotników 32/46, 02-668 Warsaw, Poland.

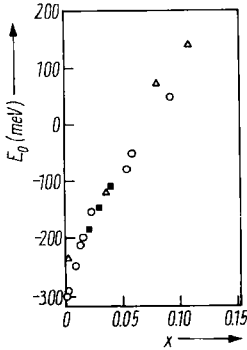


Fig. 1. The energy gap variation with composition of $\text{Hg}_{1-x}\text{Mn}_x\text{Te}$ mixed crystals: ■ our samples; ○ samples studied in magnetoabsorption experiment [11]; △ data from absorption investigation [4], the point at $E_g = -300$ meV and $x = 0$ — data for pure HgTe [12]

semimetallic at low x -values; at $x = 0.07$ a semimetal–semiconductor transition occurs at 4.2 K and increasing the value of x still further we enter into the region of semiconducting band ordering.

On the other hand, the behaviour of $\text{Hg}_{1-x}\text{Mn}_x\text{Te}$ mixed crystals in the presence of strong quantizing magnetic fields and at low temperatures cannot be understood in terms of the usual models.

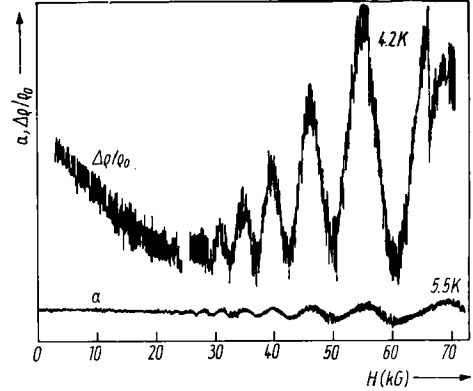
This paper presents the results of the quantum transport phenomena investigations. The aim of this work was to obtain a more detailed information on the band structure in strong magnetic fields. For this purpose we measured the Shubnikov-de Haas (ShdH) effect and it turned out that neither the three-band model [8] nor the Pidgeon-Brown model [9] can explain the observed phenomena. Namely, for any set of parameters the positions of the ShdH maxima did not fit the energy band scheme as calculated according to these models. Moreover, the position of the maxima in magnetic field turned out to be strongly temperature dependent, while in the above-mentioned models they were relatively insensitive to temperature. The spin splitting was found to be very large, about three times larger than the values predicted by usual models. The amplitude of ShdH oscillations turned out to be a non-monotonic function of the temperature, contradictory to the existing theories of the ShdH effect. These facts made us think that the band structure of $\text{Hg}_{1-x}\text{Mn}_x\text{Te}$ in a quantizing magnetic field differs considerably from the band structure of an ordinary narrow-gap semiconductor. This hypothesis is also supported by recent studies on the infrared interband magnetoabsorption in this material [10, 11]. The results of the latter experiments also could not be explained in terms of the usual theoretical approaches.

In order to explain the experimental data we included into the Pidgeon-Brown model the exchange interaction between conduction electrons and electrons from Mn 3d shells. This interaction modifies considerably the usual band structure and it accounts well for all observed phenomena. Essentially the same model made possible the interpretation of magnetoabsorption experiments [11].

2. Experimental Details

The mixed crystals of $\text{Hg}_{1-x}\text{Mn}_x\text{Te}$ were grown by the modified Bridgman method and by traveling zone technique. The compositions of our samples as determined by the density measurements and microprobe analysis were equal to $x = 0.02, 0.03$, and 0.04 , and were higher than in the case of magneto-optical experiments [11] where samples with $x \leq 0.015$ were studied. The samples were n-type and the electron con-

Fig. 2. Experimental traces of oscillatory magnetoresistance (upper curve) and thermoelectric power (lower curve) in $\text{Hg}_{0.98}\text{Mn}_{0.02}\text{Te}$ sample with $n = 7.5 \times 10^{17} \text{ cm}^{-3}$ (dc technique)



centration ranged from 10^{15} cm^{-3} (pure samples) to 10^{18} cm^{-3} (gallium doped samples). We measured the Shubnikov-de Haas effect in the longitudinal as well as in the transverse configuration. Both standard dc technique and low-field modulation method were used. The experiments were performed in a superconducting magnet providing fields up to 70 kG. Preliminary measurements were also carried out in pulsed fields up to 300 kG. The temperature of the measurements ranged from 2 up to 25 K. The thermoelectric power in quantizing magnetic fields was also measured. In the case of doped samples its behaviour was also of oscillatory nature. These oscillations were compatible with the ShdH oscillations, the extrema were positioned at the same values of the magnetic field (see Fig. 2).

3. Theoretical Model

As it was mentioned above the usual theoretical descriptions [8, 9] of the band structure of narrow-gap semiconductors in magnetic field are not sufficient to explain our experimental data, neither qualitatively nor quantitatively. Although these models were constructed for a semiconductor with a periodic lattice, their validity can be extended also to semiconducting mixed crystals by means of virtual crystal approximation. This extension proved to be successful in the case of several mixed crystals, e.g., $\text{Hg}_{1-x}\text{Cd}_x\text{Te}$ [13] or $\text{Hg}_{1-x}\text{Cd}_x\text{Se}$ [14]. However, the method of virtual crystal approximation cannot be applied to the highly localized 3d electrons of manganese ions in our case. Therefore, one may suspect that the presence of these electrons is the source of discrepancies between theoretical predictions and our results. A necessity then arises to include the interaction between conduction electrons and 3d electrons of manganese ions into the theoretical model. It is an exchange interaction commonly called s-d interaction [15]. The electrons from the half-filled 3d shell of manganese form the total spin of an ion and produce magnetic moments localized on Mn. Therefore, they are responsible for the magnetic properties of $\text{Hg}_{1-x}\text{Mn}_x\text{Te}$ crystals, for instance, for the magnetization of the samples. We shall describe the system of 3d electrons in terms of the total spin of manganese ion S_n . It was proved in EPR experiments [16] that in the case of Mn ions in HgTe the total spin is $S = \frac{5}{2}$.

The s-d exchange interaction was frequently considered when describing the scattering by spin fluctuations in magnetic semiconductors or the shift of the band edges in these materials [17].

As it was shown in [18] in the case of $\text{Hg}_{1-x}\text{Mn}_x\text{Te}$ the s-d exchange interaction has the usual form

$$H_I = \sum_{\mathbf{R}_n} J(\mathbf{r} - \mathbf{R}_n) \boldsymbol{\sigma} \cdot \mathbf{S}_n, \quad (1)$$

where $\boldsymbol{\sigma}$ is the spin operator of an electron, \mathbf{S}_n is the total spin operator of the manganese ion at \mathbf{R}_n , $J(\mathbf{r})$ is the corresponding exchange integral. This Hamiltonian gives rise to several additional matrix elements in the usual basis, convenient to describe the situation of a narrow-gap semiconductor of zincblende structure. We choose this basis as in [9]:

$$\left. \begin{aligned} u_{10} &= |S\uparrow\rangle, \\ u_{20} &= |iS\downarrow\rangle, \\ u_{30} &= \left| \frac{1}{\sqrt{2}} (X + iY)\uparrow \right\rangle, \\ u_{40} &= \left| i \frac{1}{\sqrt{2}} (X - iY)\downarrow \right\rangle, \\ u_{50} &= \left| \frac{1}{\sqrt{6}} [(X - iY)\uparrow + 2Z\downarrow] \right\rangle, \\ u_{60} &= \left| i \frac{1}{\sqrt{6}} [(X + iY)\downarrow - 2Z\uparrow] \right\rangle, \\ u_{70} &= \left| i \frac{1}{\sqrt{3}} [-(X - iY)\uparrow + Z\downarrow] \right\rangle, \\ u_{80} &= \left| \frac{1}{\sqrt{3}} [(X + iY)\downarrow + Z\uparrow] \right\rangle, \end{aligned} \right\} \quad (2)$$

where S, X, Y, Z are lattice-periodic functions which transform as s, p_x, p_y, p_z functions under transformations of the T_d point group. In this basis the matrix elements of (1) form an 8×8 matrix D' where α and β are new material constants describing the exchange interaction defined as

$$\left. \begin{aligned} \alpha &= \langle S | J | S \rangle, \\ \beta &= \langle X | J | X \rangle, \end{aligned} \right\} \quad (3)$$

and $S^\pm = S_x \pm iS_y$, S_z are the components of manganese total spin. N_s denotes the number of manganese ions in the crystal lattice.

$$D' = \begin{pmatrix} \frac{1}{2} N_s \alpha S_z & \frac{i}{2} N_s \alpha S^- & 0 & 0 & 0 & 0 & 0 & 0 \\ -\frac{i}{2} N_s \alpha S^+ & -\frac{1}{2} N_s \alpha S_z & 0 & 0 & 0 & 0 & 0 & 0 \\ 0 & 0 & \frac{1}{2} N_s \beta S_z & 0 & 0 & \frac{i}{2\sqrt{3}} N_s \beta S^- & 0 & \frac{1}{\sqrt{6}} N_s \beta S^- \\ 0 & 0 & 0 & -\frac{1}{2} N_s \beta S_z & -\frac{i}{2\sqrt{3}} N_s \beta S^+ & 0 & -\frac{1}{\sqrt{6}} N_s \beta S^+ & 0 \\ 0 & 0 & 0 & \frac{i}{2\sqrt{3}} N_s \beta S^- & -\frac{1}{6} N_s \beta S_z & -\frac{i}{3} N_s \beta S^+ & \frac{i\sqrt{2}}{3} N_s \beta S_z & \frac{\sqrt{2}}{6} N_s \beta S^+ \\ 0 & 0 & -\frac{i}{2\sqrt{3}} N_s \beta S^+ & 0 & \frac{i}{3} N_s \beta S^- & \frac{1}{6} N_s \beta S_z & \frac{i\sqrt{2}}{6} N_s \beta S^- & \frac{i\sqrt{2}}{3} N_s \beta S_z \\ 0 & 0 & 0 & -\frac{1}{\sqrt{6}} N_s \beta S^- & \frac{i\sqrt{2}}{3} N_s \beta S_z & -\frac{i\sqrt{2}}{6} N_s \beta S^+ & \frac{1}{6} N_s \beta S_z & -\frac{i}{6} N_s \beta S^+ \\ 0 & 0 & \frac{1}{\sqrt{6}} N_s \beta S^+ & 0 & \frac{\sqrt{2}}{6} N_s \beta S^- & -\frac{i\sqrt{2}}{3} N_s \beta S_z & \frac{i}{6} N_s \beta S^- & -\frac{1}{6} N_s \beta S_z \end{pmatrix} \quad (4)$$

In order to find the energies of conduction and valence electrons we have to solve the following determinantal equation:

$$\det |D + D' - I\lambda| = 0, \quad (5)$$

where D is an 8×8 matrix which is given in three-band approximation in [8], or including the interaction with higher bands in [9]. For the case of $k_z \neq 0$ the matrix D is given, e.g., in [19]. Such general form of eigenvalue problem is very difficult to solve. The usual form of electron wave functions involving only few harmonic oscillator functions is not adequate in this case. Even in the $k_z = 0$ case equation (5) does not separate into two 4×4 matrices corresponding to a- and b-sets of energy levels. Moreover, the off-diagonal terms couple the electron states with the states of manganese spins, thus increasing the complexity of the problem. To make the problem solvable we performed a thermal average of D' with respect to the Mn spins. This simplified considerably the matrix D' since $\langle S^+ \rangle = \langle S^- \rangle = 0$ (for low values of x which is the case in this study, $\text{Hg}_{1-x}\text{Mn}_x\text{Te}$ does not exhibit a magnetic ordered phase [2, 3]). This approximation is in close analogy to the effective field approximation commonly used in the theory of magnetism [20]. It is even more justified in our case because the conduction electron being a mobile carrier interacts with a great number of manganese spins. In such an approximation D' decouples into 4×4 matrices which correspond to a-set and b-set of the Pidgeon and Brown model (D also decouples into D_a and D_b 4×4 matrices in this case):

$$D'_a = \begin{pmatrix} \frac{1}{2} N_s \alpha \langle S_z \rangle & 0 & 0 & 0 \\ 0 & \frac{1}{2} N_s \beta \langle S_z \rangle & 0 & 0 \\ 0 & 0 & -\frac{1}{6} N_s \beta \langle S_z \rangle & -\frac{i\sqrt{2}}{3} N_s \beta \langle S_z \rangle \\ 0 & 0 & \frac{i\sqrt{2}}{3} N_s \beta \langle S_z \rangle & \frac{1}{6} N_s \beta \langle S_z \rangle \end{pmatrix} \quad (6)$$

(basis functions $u_{10}, u_{30}, u_{50}, u_{70}$),

$$D'_b = \begin{pmatrix} -\frac{1}{2} N_s \alpha \langle S_z \rangle & 0 & 0 & 0 \\ 0 & \frac{1}{6} N_s \beta \langle S_z \rangle & 0 & \frac{i\sqrt{2}}{3} N_s \beta \langle S_z \rangle \\ 0 & 0 & -\frac{1}{2} N_s \beta \langle S_z \rangle & 0 \\ 0 & -\frac{i\sqrt{2}}{3} N_s \beta \langle S_z \rangle & 0 & -\frac{1}{6} N_s \beta \langle S_z \rangle \end{pmatrix} \quad (7)$$

(basis functions $u_{20}, u_{60}, u_{40}, u_{80}$).

In further calculations we neglected also the off-diagonal terms in D'_a, D'_b . These terms are coupling the spin-orbit split-off band of Γ_7 symmetry. Since the value of spin-orbit splitting is relatively large, this approximation does not cause great errors when the energy of conduction electrons is concerned.

In principle we can now solve our eigenvalue problem treating α and β as adjustable parameters. The thermal average of the z -component of manganese spin $\langle S_z \rangle$ which also appears in D'_a and D'_b is proportional to the magnetization of the sample and, therefore, could be deduced from the experimental data concerning this quantity. For this purpose the knowledge of temperature and magnetic field dependence of magnetization is necessary. Unfortunately the data available are not sufficient. There are two possible ways to overcome this problem. One can either treat $\langle S_z \rangle$ as a fitting parameter or calculate the values of this quantity within some theoretical model. The first possibility was chosen by Bastard et al. [11], while we followed the second alternative. In the approximation of non-interacting magnetic moments we have

$$\langle S_z \rangle = -\frac{5}{2} B_{5/2}(Z); \quad Z = \frac{g\mu_B SH}{k_B T}, \quad (8)$$

where $B_S(Z)$ is the Brillouin function

$$B_S(Z) = \frac{2S+1}{2S} \coth\left(\frac{2S+1}{2S} Z\right) - \frac{1}{2S} \coth\left(\frac{Z}{2S}\right). \quad (9)$$

The Landé factor g of the manganese ion can be taken as equal to 2.0 with a very good accuracy [16].

However, a considerable deviation from the Brillouin law is observed [2, 3]. Therefore, we included also the contribution of manganese pairs, which can be found due to a random distribution of Mn ions in the crystal lattice. The exchange interaction of magnetic moments within such a pair cannot be neglected. We assumed that this interaction is of Heisenberg type $H_p = I \mathbf{S}_1 \cdot \mathbf{S}_2$, where I is the appropriate exchange constant. In this model the following formula is obtained:

$$\begin{aligned} \langle S_z \rangle = & -\frac{5}{2} B_{5/2}(Z) (1-x)^{12} - 6x(1-x)^{18} \times \\ & \times \frac{\sum_{s=0}^5 \sum_{m=-s}^s m \exp\left[-\frac{g\mu_B m H}{k_B T}\right] \exp\left[-\frac{IS(S+1)}{2k_B T}\right]}{\sum_{s=0}^5 \sum_{m=-s}^s \exp\left[-\frac{g\mu_B m H}{k_B T}\right] \exp\left[-\frac{IS(S+1)}{2k_B T}\right]}. \end{aligned} \quad (10)$$

The factors $(1-x)^{12}$ and $6x(1-x)^{18}$ are the probabilities of finding an isolated manganese ion (with no Mn as nearest neighbours) and a pair of manganese ions, in the f.c.c. lattice, respectively. The value of exchange constant I was found by fitting the above model to the experimental magnetization of $\text{Hg}_{0.99}\text{Mn}_{0.01}\text{Te}$ sample. The fit is shown in Fig. 3. We found that $I = 0.7$ meV and we used this value to calculate $\langle S_z \rangle$ for $x = 0.02, 0.03$, and 0.04 . This model is, of course, rather crude and may be a source of discrepancies between our ShdH data and theoretical calculations.

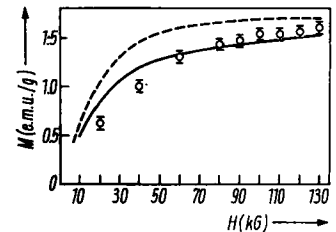


Fig. 3. The magnetization of $\text{Hg}_{0.99}\text{Mn}_{0.01}\text{Te}$ sample at 4.2 K (○). The upper curve was calculated assuming that Mn moments do not interact with each other. The lower curve was obtained by fitting to equation (10)

The wave functions of conduction and valence electrons can be chosen in such a way as to be proportional to harmonic oscillator functions, similarly as in the case of the usual Pidgeon-Brown model. Therefore, for instance, the selection rules of magneto-optical transitions remain unchanged. One can also use the notation of the Pidgeon-Brown model to label the electronic states.

In principle one can add D'_a , D'_b to the simpler three-band model matrix and find the eigenvalues. However, in this case even the three-band model has to be solved numerically. Moreover, the Luttinger quantum effects are not included in this model and, therefore, our ShdH and magnetoabsorption [11] data are better described if D'_a , D'_b are added to the Pidgeon-Brown matrices.

4. Comparison with Experiment

Using the theoretical model outlined in the previous section we calculated the electron energy levels in $\text{Hg}_{1-x}\text{Mn}_x\text{Te}$ and treating α and β as adjustable parameters fitted this calculation to the experimental ShdH data. The values of other parameters describing the conduction band were obtained from the temperature behaviour of oscillation amplitudes. Since the amplitude proved to be a non-monotonic function of temperature one may doubt whether this is possible at all. Nevertheless, in the temperature region 20 to 25 K the amplitude behaves in an ordinary way and this enabled us to estimate the values of energy gap E_0 and momentum matrix element P . The details of these calculations will be dealt with in a paper to follow [21]. The remaining parameters were taken as for pure HgTe crystals. The values of all parameters used by us are listed in Table 1. The values of α and β obtained by the fitting procedure are $\alpha = -0.7$ eV and $\beta = 1.4$ eV. The fit was only weakly sensitive to the actual choice of α . This is, of course, due to the fact that in the ShdH experiment we studied only the conduction electron levels. The wave functions of these electrons are in our case mainly of p-type, i.e. sensitive to the parameter β . Therefore, we took in further calculations

Table 1
The parameters used in our calculations

x	0.02	0.03	0.04	ref.
energy gap $E_0 = E_{\Gamma_6} - E_{\Gamma_8}$ (eV) at 4.2 K	-0.187	-0.147	-0.108	[21]
momentum matrix element P (10^{-8} eV cm)	8.2	8.1	8.0	[21]
higher band parameters				
F		0		[25]
γ_1		3.0		[25]
γ_2		-0.5		[25]
γ_3		0.67		[25]
κ		-1.3		[25]
spin-orbit splitting Δ (eV)		1.08		[25]
exchange constants				
α (eV)		-0.7		[11]
β (eV)		1.4		this work

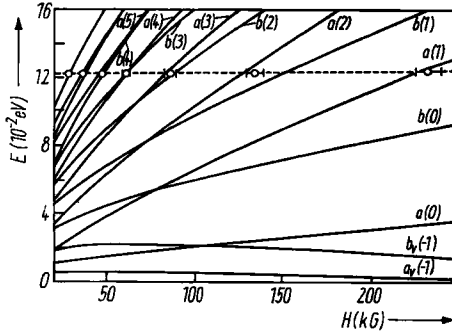


Fig. 4

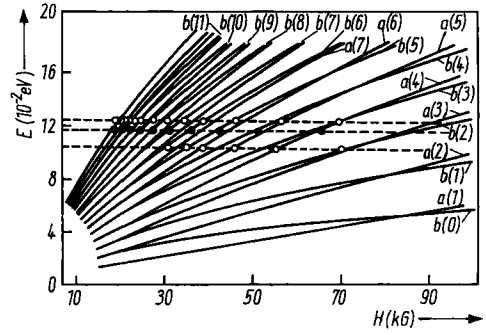


Fig. 5

Fig. 4. The calculated energy levels of conduction electrons in $\text{Hg}_{0.98}\text{Mn}_{0.02}\text{Te}$ at 4.2 K. The dashed line represents the Fermi level of the sample with $n = 7.5 \times 10^{17} \text{ cm}^{-3}$. Points represent the positions of ShdH peaks (pulsed-field experiment)

Fig. 5. Comparison between theoretical and experimental positions of ShdH peaks for three $\text{Hg}_{0.98}\text{Mn}_{0.02}\text{Te}$ samples at 4.2 K with electron concentration $n = 8.5 \times 10^{17}$, 7.8×10^{17} , and $6.5 \times 10^{17} \text{ cm}^{-3}$

the value of the ratio $\alpha/\beta = -0.5$ as obtained in [11]. The value of β obtained by us is in good agreement with $\beta = 1.5 \text{ eV}$ found in [11]. The fit was more sensitive to the choice of β in the case of samples with electron concentration of the order of 10^{15} cm^{-3} . In doped samples the Fermi level was lying considerably higher and the exchange corrections are of less importance (though appreciable) in this case. Fig. 4 to 7 present the comparison of our model with experiments for some of $x = 0.02$ and 0.4 doped samples at various temperatures. The agreement seems to be quite satisfactory. As it can be observed in Fig. 4 the sequence of the levels belonging to a- and b-sets is reversed in magnetic fields up to 75 kG. For stronger magnetic fields the ordering of the levels is usual as in ordinary narrow-gap semiconductors. A very interesting fact can also be observed in Fig. 4, namely the valence band level $b_v(-1)$ is lying higher in energy than the lowest conduction band level $a(0)$ below 100 kG. This suggests that at lower fields we are dealing with an overlap of the bands and above this value of

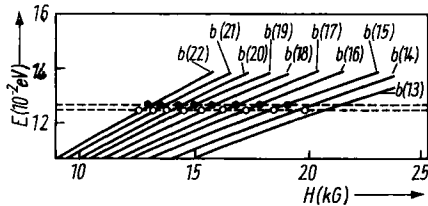


Fig. 6

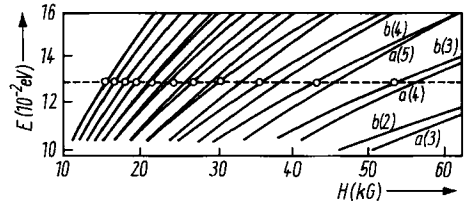


Fig. 7

Fig. 6. Comparison between theoretical and experimental ShdH peak positions for $\text{Hg}_{0.98}\text{Mn}_{0.02}\text{Te}$ with $n = 8.5 \times 10^{17}$ and $7.8 \times 10^{17} \text{ cm}^{-3}$ at 8.9 K (low-field modulation technique). The levels denoted have closely lying $b(n)$ and $a(n - 1)$ levels

Fig. 7. SdH peak positions for $\text{Hg}_{0.96}\text{Mn}_{0.04}\text{Te}$ sample with $n = 6.1 \times 10^{17} \text{ cm}^{-3}$ at 4.2 K compared with theoretical calculations

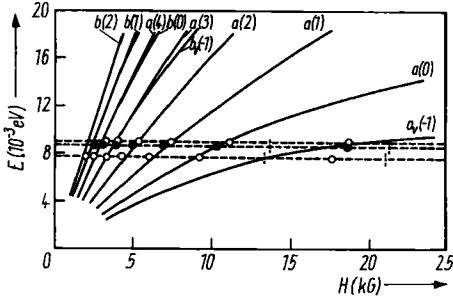


Fig. 8

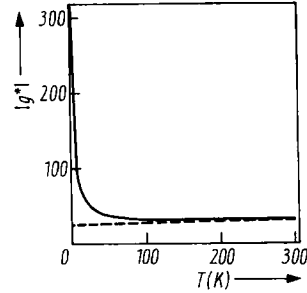


Fig. 9

Fig. 8. ShdH peak positions for $\text{Hg}_{0.97}\text{Mn}_{0.03}\text{Te}$ samples with $n = 4.7 \times 10^{15}$, 4.6×10^{16} , $3.5 \times 10^{15} \text{ cm}^{-3}$ at 4.2 K. The points in the vicinity of the $a_v(-1)$ level represent ShdH peaks observed in longitudinal magnetoresistance. The splitting of these peaks in transverse configuration is marked with vertical bars

Fig. 9. Electronic g -factor calculation for the $N = 15$ Landau level at 10 kG for $\text{Hg}_{0.98}\text{Mn}_{0.02}\text{Te}$ according to our model (full line) and the usual Pidgeon-Brown theory (dashed line)

magnetic field the real energy gap opens. The transitions into $b_v(-1)$ level were in fact seen in magneto-optical experiment [11]. The value of magnetic field at which the crossing of the $b_v(-1)$ and $a(0)$ levels occurs depends both on the temperature and composition of the crystals. At higher temperatures the crossing takes place in a smaller magnetic field, since $\langle S_z \rangle$ is a decreasing function of temperature; while comparing the results at various temperatures one can observe that the position of ShdH maxima is strongly temperature dependent. This is also due to the dependence of $\langle S_z \rangle$ on temperature. Let us also point out that the value of the spin splitting, i.e. the distance between $a(n)$ and $b(n)$ levels, is very large due to the exchange interaction leading to very large values of the g -factor at low temperatures (see Fig. 9). The comparison of theory and experiments performed on pure samples with electron concentration of the order of 10^{15} cm^{-3} is shown in Fig. 8.

We observe an additional ShdH peak due to $b_v(-1)$ level. In the neighbourhood of the $a_v(-1)$ level we observed a strange additional peak, which in the transverse configuration splits into two components. The value of this splitting is not compatible with the spin splitting of higher-lying levels. Of course, the assumption which we make throughout that the Fermi level is constant cannot be justified in this region of magnetic fields. The origin of this strange peak is perhaps connected with acceptor levels detected in magneto-optical experiments [11] and which are supposed to split in the magnetic field [22]. The detail discussion of the Fermi level behaviour with magnetic fields for $H > 10 \text{ kG}$ in Fig. 8 needs to extend the theory. The shapes of the magnetic levels $E(k_z)$ have to be calculated, then the density of states on each level, and finally the Fermi level versus magnetic field.

In the present moment we are not in position to give univocal explanations of the observed peaks at 18 kG in Fig. 8. A further study of this phenomenon is necessary.

Although the oscillations are no longer periodic in $1/H$, since the period in our case depends on H through the magnetic field dependence of $\langle S_z \rangle$, we were able to estimate the value of the Fermi level in our samples. In the region of magnetic fields, where the Fermi level is magnetic field independent, the peak positions univocally determine the value of the Fermi energy. This value agreed within 20% limits with the Fermi level obtained by Hall coefficient experiments at low magnetic fields. As it

was mentioned the energy levels are strongly temperature dependent through $\langle S_z \rangle$. This leads to the variation of electron g -factors with the temperature, Fig. 9. At higher temperatures g -factors return to the value obtained on the basis of usual theories. This g -factor temperature dependence helps to understand the most striking effect detected in our experiments, namely the non-monotonic variation of the oscillation amplitude with temperature. The existing theories of the ShdH effect [25] predict that the amplitude should be a monotonically decreasing function of temperature. For example, for the transverse configuration we have the following expression:

$$A = \sum_{R=1}^{\infty} (-1)^R \frac{5}{2} \left(\frac{Re}{\hbar c H} \right)^{1/2} \frac{BTm' \cos(\pi R m' g/2) \cos 2\pi(R \hbar c k_F^2 / 2eH - 1/8)}{\sinh(RBTm'/H) \exp(RBT_D m'/H)}, \quad (11)$$

$$B = \frac{2\pi^2 k_0 c m_0}{\hbar e}, \quad (12)$$

T_D being Dingle temperature. Usually the first term, $R = 1$, suffices to describe the temperature dependence of the amplitude.

However, it turned out in our experiments that the amplitude drops to a very small value at a certain temperature T_{\min} (see, e.g., Fig. 10a, b) while it is significant in the vicinity of T_{\min} . The value of T_{\min} depends both on composition and electron concentration of the sample.

Expression (11) for the amplitude contains a cosine term. It may drop to zero if its argument is equal to an odd integer times $\pi/2$ thus suppressing the amplitude. If we insert in (11) the values of g -factors calculated according to our model, which are now temperature dependent, we can achieve a good agreement with the observations (see Fig. 10). These calculations took into account the first three terms in (11). However, the situation looks more complicated in the case of doped samples, which is shown in Fig. 11 and 12. The cosine term oscillates more rapidly in this case giving rise to a series of zeros of the amplitude. The uncertainties of the temperature measurement make it impossible to state whether the theory agrees with experiment or not. It must be said that these calculations are extremely sensitive to the values of the parameters α and β and also to the composition of the crystal. The values of these parameters are not known accurately enough to check the validity of the theory. A non-monotonic behaviour of the ShdH effect amplitude was also observed by Morrissy [24]

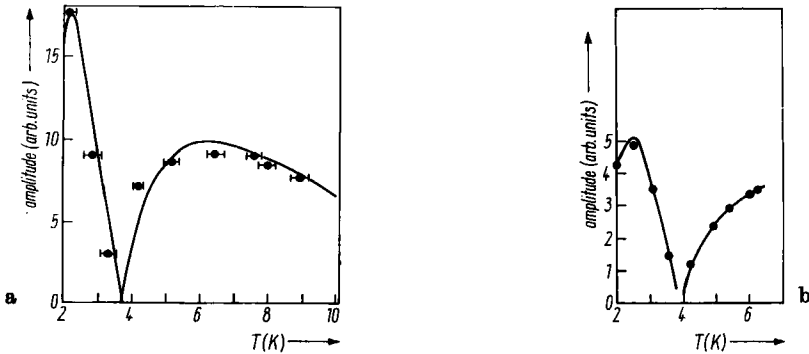


Fig. 10. The normalized amplitude of ShdH oscillations for a) $\text{Hg}_{0.98}\text{Mn}_{0.02}\text{Te}$, $n = 4.0 \times 10^{15} \text{ cm}^{-3}$ and b) $\text{Hg}_{0.97}\text{Mn}_{0.03}\text{Te}$, $n = 4.0 \times 10^{15} \text{ cm}^{-3}$. The line was calculated (see text)

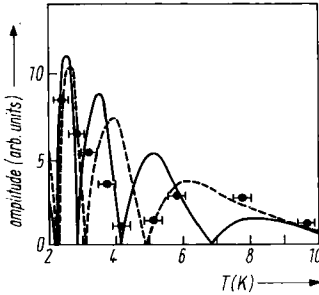


Fig. 11

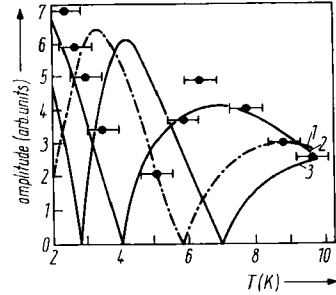


Fig. 12

Fig. 11. Normalized ShdH oscillation amplitude for $\text{Hg}_{0.98}\text{Mn}_{0.02}\text{Te}$ with $n = 8.5 \times 10^{17} \text{ cm}^{-3}$ (points). The lines were calculated with the parameters corresponding to $x = 0.02$ (full line) and $x = 0.025$ (dashed line)

Fig. 12. Normalized ShdH oscillation amplitude for $\text{Hg}_{0.98}\text{Mn}_{0.02}\text{Te}$ with $n = 8.5 \times 10^{17} \text{ cm}^{-3}$ for various α . (1) $\alpha = -0.7$; (2) -1.0 ; (3) -0.5 eV ; $\beta = 1.4 \text{ eV}$

in $\text{Hg}_{0.9}\text{Mn}_{0.1}\text{Te}$. The phases of the oscillations at both sides of T_{\min} should, of course, differ by π . This was in fact observed unambiguously in the case of pure samples, the only exception being again the strange peak lying near $a_v(-1)$ level.

5. Concluding Remarks

$\text{Hg}_{1-x}\text{Mn}_x\text{Te}$ mixed crystals seem to belong to a new well distinguished group of materials, which could be called "semimagnetic semiconductors". The anomalous behaviour of these mixed crystals in quantizing magnetic fields and at low temperatures distinguishes these materials from usual narrow-gap semiconductors. These anomalies are due to the exchange interaction between conduction and valence electrons and highly localized 3d electrons of magnetic manganese ions. The absence of a magnetic ordered phase and the random distribution of Mn ions in the lattice make the properties of these crystals different also from typical magnetic semiconductors. Nevertheless the exchange effects can be observed even at very low content of Mn ions in the crystal lattice. There are some properties of these crystals (such as the very high mobility $\mu > 10^6 \text{ cm}^2/\text{V s}$ of electrons at low temperatures) which are still waiting to be explained. We should like also to point out that in the case of usual magnetic semiconductors a very complicated band structure, if known at all, made the study of exchange interactions between mobile carriers and localized magnetic moments a particularly difficult task. On the other hand, the band structure of $\text{Hg}_{1-x}\text{Mn}_x\text{Te}$ in the absence of a magnetic field seems to be well described in Kane's theory. Therefore, semimagnetic semiconductors offer a unique possibility of detailed investigation concerning exchange s-d interaction. On the other hand, the semiconducting properties can be strongly influenced by controlling the magnetic properties of the crystals. We expect that $\text{Hg}_{1-x}\text{Mn}_x\text{Se}$, $\text{Cd}_{1-x}\text{Mn}_x\text{Te}$, etc. will belong to the same group of materials.

Acknowledgements

We are indebted to Dr. P. Byszewski for letting us perform the pulsed-field experiments in his laboratory. We are grateful to Dr. J. Mycielski, Dr. G. Bastard, Dr. W. Walukiewicz, Dr. L. Leibler, and Dr. W. Dobrowolski for many helpful discussions. The help of Dr. W. Dobrowolski in performing numerical calculations is acknowledged. A part of the samples was obtained from Dr. W. Girit to whom we wish to express our thanks.

References

- [1] R. T. DELEVES and B. LEWIS, J. Phys. Chem. Solids **24**, 549 (1963).
- [2] H. SAVAGE, J. J. RHYNE, R. HOLM, J. R. CULLEN, C. E. CARROL, and E. P. WOHLFARTH, phys. stat. sol. (b) **58**, 685 (1973).
- [3] D. ADRIANOV, F. GIMELFARB, P. KUSHNIR, I. LOPATINSKII, M. PASHKOVSKII, A. SAVELEV, and V. FISTUL, Fiz. Tekh. Poluprov. **10**, 111 (1976).
- [4] J. KANIEWSKI, Ph. D. Thesis, Institute of Physics, Polish Academy of Sciences, Warsaw 1976 (unpublished).
- [5] J. STANKIEWICZ, W. GIRIAT, and M. V. BIEN, phys. stat. sol. (b) **68**, 485 (1975).
- [6] F. F. KHARAKHORIN, R. V. LUTZIV, M. V. PASHKOVSKII, and V. M. PETROV, phys. stat. sol. (a) **5**, 69 (1971).
- [7] E. O. KANE, in: Semiconductors and Semimetals, Vol. 1, Ed. R. K. WILLARDSON and A. C. BEER, Academic Press, 1966 (p. 75).
- [8] P. KACMAN and W. ZAWADZKI, phys. stat. sol. (b) **47**, 629 (1971).
- [9] C. PIDGEON and R. BROWN, Phys. Rev. **146**, 575 (1966).
- [10] G. BASTARD, C. RIGAU, and A. MYCIELSKI, phys. stat. sol. (b) **79**, 585 (1977).
- [11] G. BASTARD, C. RIGAU, Y. GULDNER, J. MYCIELSKI, and A. MYCIELSKI, J. Physique **39**, 87 (1978).
- [12] G. BASTARD, Proc. III. Internat. Conf. Phys. Narrow-Gap Semicond., Warsaw 1977, to be published.
- [13] Y. GULDNER, C. RIGAU, A. MYCIELSKI, and Y. COUDER, phys. stat. sol. (b) **81**, 615 (1977).
- [14] W. DOBROWOLSKI and T. DIETL, Proc. XIII. Internat. Conf. Phys. Semicond., Rome 1976 (p. 447).
- [15] T. KASUYA, Progr. Theor. Phys. (Kyoto) **16**, 45 (1956).
- [16] K. LEIBLER, W. GIRIAT, Z. WILAMOWSKI, and R. IWANOWSKI, phys. stat. sol. (b) **47**, 405 (1971).
- [17] C. HAAS, Crit. Rev. Solid State Sci. **1**, 47 (1970).
- [18] J. KOSSUT, phys. stat. sol. (b) **78**, 537 (1976).
- [19] W. LEUNG and L. LIU, Phys. Rev. B **8**, 3811 (1973).
- [20] J. S. SMART, Effective Field Theories of Magnetism, W. B. Saunders Co., Philadelphia 1966.
- [21] M. JACZYŃSKI, W. DOBROWOLSKI, and R. R. GAŁĄZKA, to be published.
- [22] P. BYSZEWSKI, K. SZLENK, and R. R. GAŁĄZKA, see [12].
- [23] L. ROTH and P. N. ARGYRES, see [7] (p. 159).
- [24] J. H. MORRISSEY, Ph. D. Thesis, Oxford University, unpublished.
- [25] S. H. GROVES, R. N. BROWN, and C. R. PIDGEON, Phys. Rev. **161**, 779 (1967).

(Received March 10, 1978)